

# Study of the radiative decay $\phi \rightarrow a_0(980)\gamma$ with the KLOE detector

The KLOE Collaboration

F. Ambrosino<sup>d</sup>, A. Antonelli<sup>a</sup>, M. Antonelli<sup>a</sup>, F. Archilli<sup>a</sup>,  
 C. Bacci<sup>h</sup>, P. Beltrame<sup>b</sup>, G. Bencivenni<sup>a</sup>, S. Bertolucci<sup>a</sup>,  
 C. Bini<sup>g</sup>, C. Bloise<sup>a</sup>, S. Bocchetta<sup>h</sup>, V. Bocci<sup>g</sup>, F. Bossi<sup>a</sup>,  
 P. Branchini<sup>h</sup>, R. Caloi<sup>g</sup>, P. Campana<sup>a</sup>, G. Capon<sup>a</sup>,  
 T. Capussela<sup>d</sup>, F. Ceradini<sup>h</sup>, S. Chi<sup>a</sup>, G. Chiefari<sup>d</sup>,  
 P. Ciambrone<sup>a</sup>, E. De Lucia<sup>a</sup>, A. De Santis<sup>g</sup>, P. De Simone<sup>a</sup>,  
 G. De Zorzi<sup>g</sup>, A. Denig<sup>b</sup>, A. Di Domenico<sup>g</sup>, C. Di Donato<sup>d</sup>,  
 S. Di Falco<sup>e</sup>, B. Di Micco<sup>h</sup>, A. Doria<sup>d</sup>, M. Dreucci<sup>a</sup>, G. Felici<sup>a</sup>,  
 A. Ferrari<sup>a</sup>, M. L. Ferrer<sup>a</sup>, G. Finocchiaro<sup>a</sup>, S. Fiore<sup>g</sup>,  
 C. Forti<sup>a</sup>, P. Franzini<sup>g</sup>, C. Gatti<sup>a</sup>, P. Gauzzi<sup>g</sup>, S. Giovannella<sup>a</sup>,  
 E. Gorini<sup>c</sup>, E. Graziani<sup>h</sup>, M. Incagli<sup>e</sup>, W. Kluge<sup>b</sup>, V. Kulikov<sup>k</sup>,  
 F. Lacava<sup>g</sup>, G. Lanfranchi<sup>a</sup>, J. Lee-Franzini<sup>a,i</sup>, D. Leone<sup>b</sup>,  
 M. Martini<sup>a</sup>, P. Massarotti<sup>d</sup>, W. Mei<sup>a</sup>, S. Meola<sup>d</sup>, S. Miscetti<sup>a</sup>,  
 M. Moulson<sup>a</sup>, S. Müller<sup>a</sup>, F. Murtas<sup>a</sup>, M. Napolitano<sup>d</sup>,  
 F. Nguyen<sup>h</sup>, M. Palutan<sup>a</sup>, E. Pasqualucci<sup>g</sup>, A. Passeri<sup>h</sup>,  
 V. Patera<sup>a,f</sup>, F. Perfetto<sup>d</sup>, M. Primavera<sup>c</sup>, P. Santangelo<sup>a</sup>,  
 G. Saracino<sup>d</sup>, B. Sciascia<sup>a</sup>, A. Sciubba<sup>a,f</sup>, F. Scuri<sup>e</sup>, I. Sfiligoi<sup>a</sup>,  
 T. Spadaro<sup>a</sup>, M. Testa<sup>g</sup>, L. Tortora<sup>h</sup>, P. Valente<sup>g</sup>,  
 B. Valeriani<sup>b</sup>, G. Venanzoni<sup>a</sup>, R. Versaci<sup>a</sup>, G. Xu<sup>a,j</sup>

<sup>a</sup>*Laboratori Nazionali di Frascati dell'INFN, Frascati, Italy.*

<sup>b</sup>*Institut für Experimentelle Kernphysik, Universität Karlsruhe, Germany.*

<sup>c</sup>*Dipartimento di Fisica dell'Università e Sezione INFN, Lecce, Italy.*

<sup>d</sup>*Dipartimento di Scienze Fisiche dell'Università "Federico II" e Sezione INFN, Napoli, Italy*

<sup>e</sup>*Dipartimento di Fisica dell'Università e Sezione INFN, Pisa, Italy.*

<sup>f</sup>*Dipartimento di Energetica dell'Università "La Sapienza", Roma, Italy.*

<sup>g</sup>*Dipartimento di Fisica dell'Università "La Sapienza" e Sezione INFN, Roma, Italy.*

<sup>h</sup>*Dipartimento di Fisica dell'Università "Roma Tre" e Sezione INFN, Roma, Italy.*

<sup>i</sup>*Physics Department, State University of New York at Stony Brook, USA.*

<sup>j</sup>*Permanent address: Institute of High Energy Physics of Academia Sinica, Beijing, China.*

<sup>k</sup>*Permanent address: Institute for Theoretical and Experimental Physics, Moscow, Russia.*

---

## Abstract

A sample of  $1.25 \times 10^9$   $\phi$  decays, collected with the KLOE detector at the Frascati  $\phi$ -factory DAΦNE at center of mass energy  $\sim M_\phi$ , has been used to study the radiative decay  $\phi \rightarrow \eta\pi^0\gamma$ . This decay is dominated by  $\phi \rightarrow a_0(980)\gamma$ . Two decay chains, corresponding to  $\eta \rightarrow \gamma\gamma$  and  $\eta \rightarrow \pi^+\pi^-\pi^0$ , have been selected. We found respectively:  $Br(\phi \rightarrow \eta\pi^0\gamma) = (6.92 \pm 0.10_{stat.} \pm 0.20_{syst.}) \times 10^{-5}$  and  $(7.19 \pm 0.17_{stat.} \pm 0.24_{syst.}) \times 10^{-5}$ . The  $\eta\pi^0$  invariant mass distributions have been fitted to obtain the relevant  $a_0(980)$  parameters.

*Key words:*  $e^+e^-$  collisions,  $\phi$  radiative decays, Scalar mesons

---

## 1 Introduction

The scalar isovector meson  $a_0(980)$ , as well as the isoscalar  $f_0(980)$ , is not easily interpreted as an ordinary  $q\bar{q}$  meson belonging to the  $^3P_0$  nonet. Alternative hypotheses have been proposed:  $q\bar{q}q\bar{q}$  states[1],  $K\bar{K}$  bound states[2], or dynamically generated resonances[3].

The radiative decay  $\phi \rightarrow \eta\pi^0\gamma$  is dominated by the exchange of the  $a_0(980)$  in the intermediate state ( $\phi \rightarrow a_0\gamma$  with  $a_0 \rightarrow \eta\pi^0$ ); the contribution of the interfering process  $\phi \rightarrow \rho^0\pi^0$  is small due to the small  $\rho^0 \rightarrow \eta\gamma$  coupling. According to the possible different structures, the branching ratio of  $\phi \rightarrow a_0\gamma$  can vary from  $10^{-5}$  in the  $q\bar{q}$  or  $K\bar{K}$  case to  $10^{-4}$  in the  $q\bar{q}q\bar{q}$  hypothesis. The mass shape is also expected to depend on the meson structure. The process has been observed and measured by SND[4] and CMD-2[5] at VEPP-2M and by KLOE[6] during its first period of data taking with limited statistics.

In this paper we present preliminary results of the analysis of the decay  $\phi \rightarrow \eta\pi^0\gamma$  performed with the KLOE detector, operated at the Frascati  $\phi$ -factory DAΦNE[11], using a sample of  $414 \text{ pb}^{-1}$  of the 2001-2002 data taking, corresponding to  $1.25 \times 10^9$   $\phi$  produced, about a factor 20 more in statistics with respect to the previous result[6]. The decay chains corresponding to  $\eta \rightarrow \gamma\gamma$  and  $\eta \rightarrow \pi^+\pi^-\pi^0$  have been selected to extract the branching ratio; the former is characterized by a higher branching ratio and large background, the latter has lower branching ratio but a smaller background contamination.

The two invariant mass spectra have then been used to evaluate the relevant  $a_0$  parameters (mass and couplings) through a combined fit.

## 2 The KLOE detector

The KLOE detector consists of a large cylindrical drift chamber[7], surrounded by a lead/scintillating-fiber sampling calorimeter[8], both immersed in a solenoidal magnetic field of 0.52 T with the axis parallel to the beams. Two small calorimeters[9] are wrapped around the quadrupoles of the low- $\beta$  insertion to complete the detector hermeticity.

The drift chamber provides a measurement of charged tracks momentum with a resolution of  $\delta p_{\perp}/p_{\perp}=0.4\%$ , and of decay vertices with an accuracy of 3 mm.

The calorimeter covers 98% of the total solid angle and provides measurements of energy, time and position of photons with accuracies of  $\sigma_E/E = 0.057/\sqrt{E}$  (GeV) and  $\sigma_t = 57 \text{ ps}/\sqrt{E} \text{ (GeV)} \oplus 50 \text{ ps}$ , respectively. A photon is defined as a cluster of energy deposits in the calorimeter not associated to a charged particle.

The trigger[10] uses information from both the calorimeter and the drift chamber. The calorimeter trigger requires two local energy deposits.

## 3 $\phi \rightarrow \eta\pi^0\gamma$ with $\eta \rightarrow \gamma\gamma$

Events from this decay chain are characterized by five prompt photons in the final state, without any charged track in the drift chamber. A prompt photon is defined as a calorimeter cluster satisfying the condition  $|t - r/c| < 5\sigma_t(E)$ , where  $r$  is the distance of the impact point on the calorimeter from the beam interaction point,  $t$  is the arrival time,  $c$  is the speed of light.

The main background processes are:

- (1)  $\phi \rightarrow \pi^0\pi^0\gamma$ , dominated by  $\phi \rightarrow f_0\gamma$
- (2)  $e^+e^- \rightarrow \omega\pi^0$  with  $\omega \rightarrow \pi^0\gamma$
- (3)  $\phi \rightarrow \eta\gamma$  with  $\eta \rightarrow \pi^0\pi^0\pi^0$
- (4)  $\phi \rightarrow \eta\gamma$  with  $\eta \rightarrow \gamma\gamma$

Events from process (3) can be wrongly reconstructed as five photon ones due to cluster merging or loss, while events from process 4 can mimic the signal due to photon splittings or to accidental clusters in the calorimeter. The background reduction proceeds through the following steps: (i) a kinematic fit on the events is performed, with the constraints of the 4-momentum conservation and  $|t - r/c| = 0$  for each prompt photon; (ii) the best photon pairing to  $\pi^0$ 's

and  $\eta$ 's is searched for in the signal and background hypotheses; and then (iii) a second kinematic fit is applied by imposing also the constraints of the masses of the intermediate particles. The  $\chi^2$  of these fits and other kinematical variables are used to cut the background events. The overall selection efficiency is 39%. The background has been evaluated on control samples dominated by the different background processes. By comparing the data with the Monte Carlo (MC) simulation of the experiment, the amount of each background, to be subtracted from the final sample, has been obtained (see fig.1, left).

The selected sample consists of 29601 events; the total background amounts

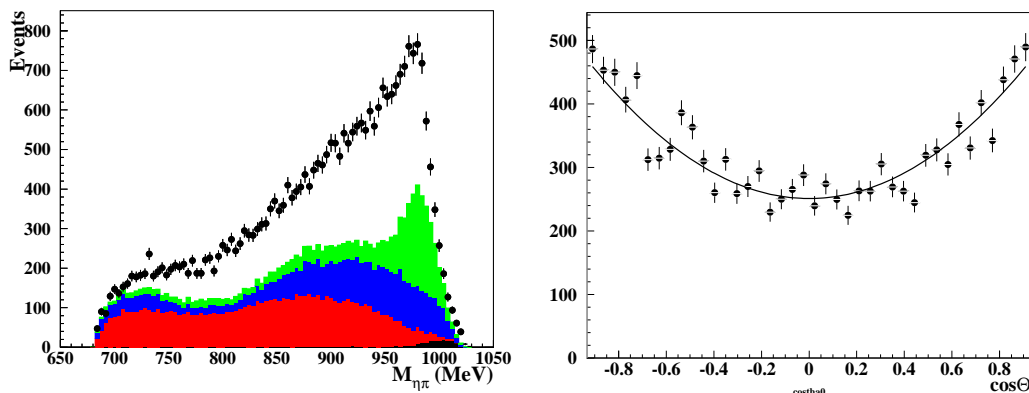


Fig. 1. Left:  $M_{\eta\pi^0}$  distribution before background subtraction; dots are data, and coloured histograms are the background contributions evaluated by MC (black:  $\phi \rightarrow \eta\gamma$  with  $\eta \rightarrow \gamma\gamma$ , blue:  $\phi \rightarrow \eta\gamma$  with  $\eta \rightarrow 3\pi^0$ , green:  $e^+e^- \rightarrow \omega\pi^0$ , red:  $\phi \rightarrow f_0\gamma$ ). Right: polar angle distribution of the recoil photon after the background subtraction.

to  $16332 \pm 86$  events, from which we extract the signal events to be  $13269 \pm 192$ . The Br is obtained by normalizing the signal counts to the number of  $\phi \rightarrow \eta\gamma$  with  $\eta \rightarrow \pi^0\pi^0\pi^0$  events selected in the same analyzed sample. We get:

$$Br(\phi \rightarrow \eta\pi^0\gamma) = (6.92 \pm 0.10_{stat.} \pm 0.20_{syst.}) \times 10^{-5} \quad (1)$$

where the first uncertainty is statistical and contains also the background subtraction contribution, while the second one is systematic and is mainly due to the error on  $Br(\phi \rightarrow \eta\gamma)$ , used in the normalization, and to the selection cuts.

In fig.1, right the distribution of the polar angle of the recoil photon (*i.e.* the non associated one) after background subtraction is also shown. The  $1 + \cos^2\Theta$  angular dependence, as expected for the radiative decay of the  $\phi$  into a scalar particle, is found.

#### 4 $\phi \rightarrow \eta\pi^0\gamma$ **with** $\eta \rightarrow \pi^+\pi^-\pi^0$

Events from this decay chain are characterized by two tracks coming from the interaction region and five prompt photons. They are selected by requiring two tracks in the drift chamber coming from a vertex close to the beam interaction point and five prompt photons, according to the definition given above. There are no other relevant processes with exactly the same final state, the background comes mainly from:

- $e^+e^- \rightarrow \omega\pi^0$  with  $\omega \rightarrow \pi^+\pi^-\pi^0$  if one additional neutral cluster is given by the background or if one of the photons splits in two clusters;
- $\phi \rightarrow K_S K_L$  with prompt  $K_L$  decay either in  $3\pi^0$  if  $K_S \rightarrow \pi^+\pi^-$  (2 tracks and 6 photons), or in  $\pi^+\pi^-\pi^0$ ,  $\pi l\nu$  if  $K_S \rightarrow \pi^0\pi^0$  (2 tracks and 6 or 4 photons): these two processes can mimic the signal either if one photon is lost or if an additional accidental cluster is identified as a photon.

The background reduction is based on kinematic fitting using as constraints the 4-momentum conservation and the  $\pi^0$  and  $\eta$  invariant masses. The overall efficiency for the signal is close to 20%, while the residual background is reduced down to approximately 15% of the signal. The latter is evaluated comparing data with MC for control samples dominated by the different background components. At the end 4180 events are selected out of which we estimate a background contamination of  $542 \pm 57$  events.

In fig.2 the  $\eta\pi^0$  raw mass spectrum of the selected events is compared to the same distribution for the estimated background.

After normalizing to  $\phi \rightarrow \eta\gamma$  with  $\eta \rightarrow \pi^0\pi^0\pi^0$  events (see above) we get the

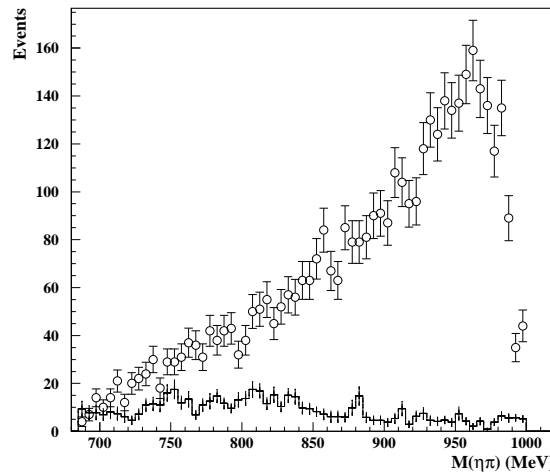


Fig. 2.  $\eta\pi^0$  raw mass spectrum of the selected events (open circles) compared to the estimated background (histogram) to be subtracted.

branching ratio:

$$Br(\phi \rightarrow \eta\pi^0\gamma) = (7.19 \pm 0.17_{stat.} \pm 0.24_{syst.}) \times 10^{-5} \quad (2)$$

where the statistical error includes the background subtraction while the systematic error is mainly due to the normalization procedure and to the efficiency evaluation.

Branching ratios (1) and (2) are independently measured apart from the common normalization. In order to compare the two measurements, we recompute the error taking away systematics due to common sources. We obtain the values:

$$\begin{aligned} Br(\phi \rightarrow \eta\pi^0\gamma) &= (6.92 \pm 0.17) \times 10^{-5} \quad (\eta \rightarrow \gamma\gamma) \\ Br(\phi \rightarrow \eta\pi^0\gamma) &= (7.19 \pm 0.24) \times 10^{-5} \quad (\eta \rightarrow \pi^+\pi^-\pi^0) \end{aligned}$$

that are in good agreement.

## 5 Fit of the invariant mass distribution

In order to extract the relevant parameters of the  $a_0(980)$  from the spectra of fig.1 and fig.2, we exploited two different models to parametrize the  $\phi \rightarrow \eta\pi^0\gamma$  amplitude:

- the “Kaon loop” (KL) model[12] in which the coupling of the  $\phi$  to the scalar mesons occurs through the formation of a charged kaon loop;
- the “No structure” (NS) model[13], in which a point-like coupling of the  $\phi$  to  $a_0\gamma$  is considered, and the scalar amplitude is parametrized as a Breit-Wigner, interfering with a polynomial background.

A combined fit of the two spectra with the same parameters has been performed. In the KL case the free parameters are: the mass of the  $a_0$ , the couplings  $g_{a_0K^+K^-}$  and  $g_{a_0\eta\pi^0}$ , the branching ratio of  $\phi \rightarrow \rho^0\pi^0 \rightarrow \eta\pi^0\gamma$  and a phase  $\delta$  between the scalar and the vector amplitudes. Another free parameter is the relative normalization between the two decay channels, *i.e.* the ratio  $Br(\eta \rightarrow \gamma\gamma)/Br(\eta \rightarrow \pi^+\pi^-\pi^0)$ . The result of the fit is shown in fig.3 while the parameters are listed in tab.1.

The number of free parameters of the NS model is larger: in addition to the same parameters of the KL fit, there are also the  $g_{\phi a_0\gamma}$  coupling and two complex parameters for the polynomial background. In order to reduce them, the  $a_0$  mass has been fixed to 983 MeV, while the  $\phi \rightarrow \rho\pi^0$  contribution has been set to the value calculated in ref.[13]. The results are plotted in fig.4 and the

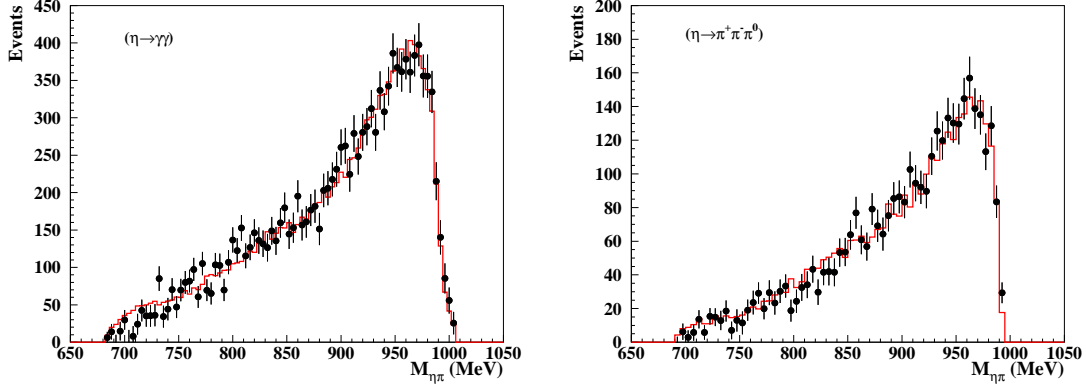


Fig. 3. Combined fit for KL model. Black points: data; solid line: fit result.

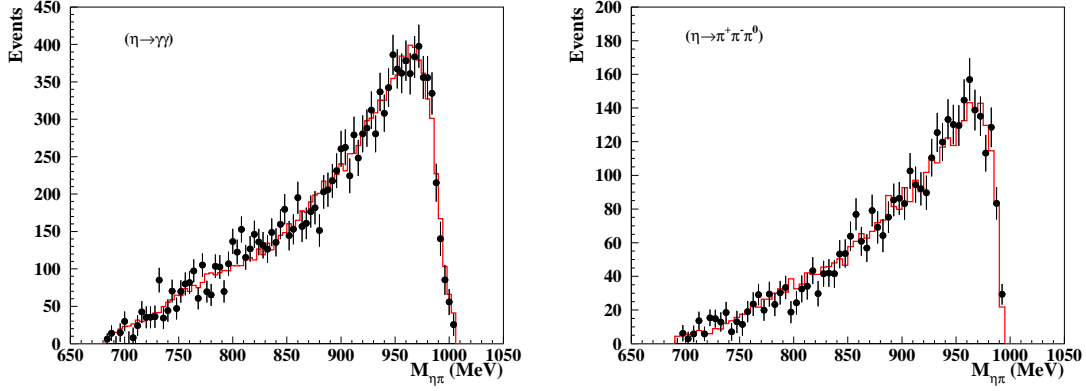


Fig. 4. Combined fit for NS model. Black points: data; solid line: fit result.

parameters values are reported in tab.1. In both fits the relative normalization turns out to be in agreement, within the quoted errors, with the world average value ( $1.73 \pm 0.03$  from PDG[14]).

## 6 Conclusions

In a sample of  $414 \text{ pb}^{-1}$  of data we have measured the branching ratio of  $\phi \rightarrow \eta \pi^0 \gamma$  selecting two different final states, corresponding to  $\eta \rightarrow \gamma \gamma$  and  $\eta \rightarrow \pi^+ \pi^- \pi^0$ . The two branching ratio values agree within the uncertainties. From the combined fit of the  $\eta \pi^0$  invariant mass distributions, we obtain the values of the relevant parameters of the  $a_0(980)$ . Large value of  $g_{a_0 K^+ K^-}$  and  $g_{\phi a_0 \gamma}$  have been found, suggesting a sizeable content of strange quark in the  $a_0(980)$ .

Table 1

Fit results (systematics on the parameters are not included).

	KL	NS
$M_{a_0}$ (MeV)	$983 \pm 1$	983 (fixed)
$g_{a_0 K^+ K^-}$ (GeV)	$2.16 \pm 0.04$	$1.57 \pm 0.13$
$g_{a_0 \eta \pi^0}$ (GeV)	$2.8 \pm 0.1$	$2.2 \pm 0.1$
$g_{\phi a_0 \gamma}$ (GeV $^{-1}$ )	—	$1.61 \pm 0.05$
$\delta(^{\circ})$	$222 \pm 12$	—
$Br(\phi \rightarrow \rho \pi^0 \rightarrow \eta \pi^0 \gamma) \times 10^6$	$0.9 \pm 0.4$	4.1 (fixed)
$Br(\eta \rightarrow \gamma \gamma)/Br(\eta \rightarrow \pi^+ \pi^- \pi^0)$	$1.69 \pm 0.04$	$1.69 \pm 0.04$
$\chi^2$	156.6	146.8
$ndf$	136	134
$P(\chi^2, ndf)$	11%	21%

## References

- [1] R.L.Jaffe, Phys. Rev. D15 (1997), 267;  
R.L.Jaffe, hep-ph/0001123.
- [2] J.Wienstein and N.Isgur, Phys.Rev.Lett. 48 (1982), 659;  
F.E.Close et al., Nucl. Phys. B389 (1993), 513;  
N.N.Achasov et al., Phys. Rev. D56 (1997), 203.
- [3] J.E.Palomar et al., Nucl.Phys. A729 (2003), 743.
- [4] M.N.Achasov et al., SND Collaboration, Phys. Lett. B479 (2000), 53.
- [5] R.R.Akhmetshin et al., CMD-2 Collaboration, Phys. Lett. B462 (1999), 380.
- [6] A.Aloisio et al., KLOE Collaboration, Phys. Lett. B536 (2002), 209.
- [7] M.Adinolfi et al., KLOE Collaboration, Nucl. Instr. and Meth. A488 (2002), 51.
- [8] M.Adinolfi et al., KLOE Collaboration, Nucl. Instr. and Meth. A482 (2002), 364.
- [9] M.Adinolfi et al., KLOE Collaboration, Nucl. Instr. and Meth. A483 (2002), 649.
- [10] M.Adinolfi et al., KLOE Collaboration, Nucl. Instr. and Meth. A492 (2002), 134.
- [11] S.Guiducci, in: P.Lucas, S.Weber (Eds.), Proceedings of the 2001 Particle Accelerator Conference, Chicago, IL, USA, 2001, p.353.
- [12] N.N.Achasov and V.N.Ivanchenko, Nucl. Phys. B315 (1989), 465;  
N.N.Achasov and A.V.Kiselev, Phys. Rev. D73 (2006), 054029.



- [13] G.Isidori et al., JHEP 0605 (2006), 049.
- [14] W.M.Yao et al., J. Phys.: Nucl. Part. Phys. G33, 1 (2006).